Abdominal Radiology (2023) 48:3585–3600
https://doi.org/10.1007/s00261-022-03757-1

SPECIAL SECTION: PET/MR

PET/MRI imaging in neuroendocrine neoplasm

Mayur K. Virarkar[1] · Matthew Montanarella[1] · Malak Itani[2] · Luis Calimano-Ramirez[1] · Dheeraj Gopireddy[1] · Priya Bhosale[3]

Received: 15 October 2022 / Revised: 22 November 2022 / Accepted: 23 November 2022 / Published online: 16 December 2022

Abstract
Molecular imaging plays a vital role in the management of neuroendocrine neoplasms (NENs). Somatostatin receptor (SSTR) PET is critical for evaluating NENs, ascertaining peptide receptor radionuclide therapy (PRRT) eligibility, and treatment response. SSTR-PET/MRI can provide a one-stop-shop multiparametric evaluation of NENs. The acquisition of complementary imaging information in PET/MRI has distinct advantages over PET/CT and MR imaging acquisitions. The purpose of this manuscript is to provide a comprehensive overview of PET/MRI and a current review of recent PET/MRI advances in the diagnosis, staging, treatment, and surveillance of NENs.

Keywords PET/MRI · Neuroendocrine neoplasm · PET/CT · PPRT · SSTR

Introduction

Neuroendocrine neoplasms (NENs) accounts for approximately 0.5% of malignancies, most commonly occurring in the gastrointestinal tract [1, 2]. Though most NENs have sporadic pathogenesis, in about 20% of cases, a familial component is recognized mainly in Multiple Endocrine Neoplasia type 1 (MEN1), Tuberous Sclerosis (TSC), Neurofibromatosis (NF) type 1, or Von Hippel Lindau (VHL) [3–5]. The overall incidence of NENs is approximately 5.86 per 100,000 per year, and 12–22% of tumors are metastatic at diagnosis [2, 3]. There was a nearly 6.4-fold increase in the prevalence of gastroenteropancreatic NENs (GEP-NENs) between 1975 and 2015, attributed to earlier detection and improved treatments with a resultant rise in survival [6]. The World Health Organization (WHO) established a set of pathological criteria to differentiate these two entities based on histologic differentiation, neuroendocrine marker expression, Ki-67 index, and mitotic activity [4, 7]. Establishing these diagnostic criteria has demonstrated a benefit in developing treatment strategies and improving the patient prognostication [8–11].

Most (> 80%) NENs share an over-expression of the somatostatin receptor (SSTR) [12]. This characteristic has shown utility in diagnostics with the advent of SSTR-PET/CT and, most recently, the PET/MRI [4]. SSTR imaging aids in the staging and development of therapeutic strategies for NENs. The European Neuroendocrine Tumor Society (ENETS) consensus guidelines recommend molecular and morphological imaging techniques for diagnosing NENs, depending on the primary tumor [13]. SSTR-PET/CT has been largely integrated into clinical practice due to the increased availability of radiotracer and PET/CT scanners, ease of image acquisition, and high accuracy for detecting NENs [1, 13, 14]. PET/MRI, a modality first introduced in 2010, has been a topic of research in recent years mainly due to the superior ability of the modality to characterize soft tissues and evaluate subtle metastatic lesions [4, 14, 15]. There are several inherent benefits regarding the use of MRI compared to CT, including a lack of ionizing radiation and superior soft tissue contrast. MRI has been established as the modality of choice for initial lesion characterization, disease staging, and assessment of treatment response for a variety of intra-abdominal solid organ malignancies. With

✉ Luis Calimano-Ramirez
luis.calimanoramirez@jax.ufl.edu

[1] Department of Radiology, University of Florida College of Medicine, Jacksonville, FL 32209, USA

[2] Mallinckrodt Institute of Radiology, Washington University in St. Louis School of Medicine, 510 S Kings Highway Blvd, Campus Box 8131, St Louis, MO 63110, USA

[3] Division of Diagnostic Imaging, Department of Diagnostic Radiology, The University of Texas MD Anderson Cancer Center, Houston, TX, USA

the addition of PET, this modality could essentially be a one-stop shop for the oncological imaging [16, 17].

The purpose of this manuscript is to provide a comprehensive overview of PET/MRI and a current review of recent PET/MRI advances in the diagnosis, staging, treatment, and surveillance of NENs.

Technical considerations in PET/MRI

In the United States, there are three manufacturers of PET/MRI machines that are available for medical use: SIGNA (GE Healthcare), uPMR 790 (United Imaging), and the Biograph mMR (Siemens) [16]. PET/MRI is a hybrid imaging technique that simultaneously acquires PET and MRI images. Each system utilizes a 3 T magnet and a lutetium scintillator. PET/MRI requires carefully selecting and administering the correct radiotracer and a collaborative effort between technologists and interpreting providers to protocol each study correctly. Based on the administering institution, there remains a range of PET/MRI acquisition parameters, the most widely used is 2 min of data acquisition per bed position [16]. High-quality coregistration following the simultaneous acquisition of imaging dataare due to advances in technical respiratory gating and motion artifact correction, owning to superior imaging quality compared to PET/CT [18–20]. Motion correction becomes increasingly essential when imaging intra-abdominally near the diaphragm because PET images are acquired during free breathing. At the same time, breath-holding is conducted during some MRI sequence acquisition [21]. Additional methods of respiratory motion reduction include MRI-based motion modeling, compressed sensing methods, and utilization of free breathing MRI sequences [21–23]. PET/MRI offers superior soft tissue characterization compared to PET/CT and even more so when the CT is acquired without IV contrast. In PET/CT, CT images are used for attenuation correction, and PET/MRI creates MR-attenuation correction images, a method that utilizes attenuation coefficient maps from acquired image data [16, 24].

A thorough review of the processes of motion and attenuation correction in the acquisition of MRI images is beyond the intended scope of this paper. Although there is some variation in NET PET/MRI imaging, protocoling can be separated into a whole-body PET/MRI protocol and a comprehensive region-specific protocol (Fig. 1). The whole-body protocol includes a multi-bed position PET acquisition. The complete protocol consists of the following sequences: axial T1 gradient recall echo (in and out of phase), axial T2 fat-saturated fast spin echo, diffusion-weighted images (up to b700), pre-contrast T1 fat-saturated, and post-contrast T1 fat-saturated. For the evaluation of liver metastasis, the focus of the MRI would be only on the liver. A partial-body PET

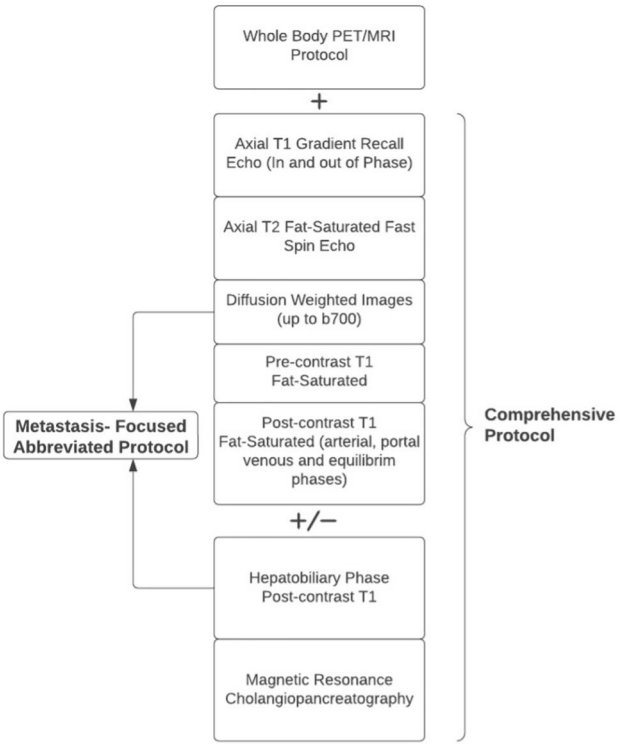

Fig. 1 Whole-body PET/MRI protocol with focused/abbreviated abdominal MRI

examination with 4–5 bed positions at 2–3 min/bed position could be performed quickly [25]. Additionally, a hepatobiliary phase post-contrast T1 sequence and magnetic resonance cholangiopancreatography (MRCP) may be obtained. An abbreviated protocol focused on metastatic disease may consist of diffusion-weighted images and hepatobiliary phase post-contrast T1 sequences [26].

PET/MRI

Several studies have examined the utility of PET/MRI in detecting NETs and metastatic disease.

Table 1 summarizes the important characteristics of studies that evaluate the role of PET–MRI in NENs (Figs. 2, 3, and 4). A dedicated meta-analysis of these prospective studies demonstrated a higher overall detection rate with the use of PET/MRI (93.5%) when compared to SSTR-PET/CT (76.8%) [14, 19, 27–30]. Specificities in detecting metastatic liver disease ranged from 95.6 to 100% for PET–MRI and 88.2% to 100% in SSTR-PET/CT [27]. This data and study confirmed general congruence in the literature on the diagnostic ability of PET/MRI in detecting NET liver metastatic lesions (Fig. 5). Studies have shown improved detection of liver metastases with MRI when a hepatobiliary contrast agent is used [31–33]. A retrospective study comparing

Table 1 Description of included PET/MRI articles

Study	Year of publication	Study design	No. of patients	Patient age mean	Total no. of liver metastases	Primary origin (*n*)	Tumor size (cm)	Type of DOTA-SSA	DOTA-SSA dose, (MBq, range)	CT for fusion	MRI for fusion	MRI magnet field (T)	DWI (*b*, s/mm^2)	MRI contrast	Fusion	PET–MRI sensitivity (%)	PET–MRI specificity (%)
Schreiter et al. [30]	2012	Prospective	24	54.8	181	Pancreas (10), ileum (5), stomach and duodenum (2), cup (1), rectum (1), lungs (1)	≤1 cm (*n* = 67) >1 cm (*n* = 76)	DOTATOC	100–120	Dyn	Dyn	1.5	*b* = 0, 100, 200, 600	HBA	Retrospective	91.2	95.6
Hope et al. [19]	2015	Prospective	10	62	101	NA	≤1 cm (*n* = 63) >1 cm (*n* = 38)	DOTATOC	179 (125–207)	PV only	Dyn	3.0	*b* = 0, 50, 600	HBA	Simultaneous	62	NA
Berzaczy et al. [28]	2017	Prospective	28	62	83	Small bowel (15), pancreas (7), colon (2), lung (1), parotid (2), CUP (1)	NA	DOTANOC	165	Dyn	Dyn	3.0	NA	HBA	Simultaneous	89.8	100

Table 1 (continued)

Study	Year of publication	Study design	No. of patients	Patient age mean	Total no. of liver metastases	Primary origin (*n*)	Tumor size (cm)	Type of DOTA-SSA	DOTA-SSA dose, (MBq, range)	CT for fusion	MRI for fusion	MRI magnet field (T)	DWI (b, s/mm^2)	MRI contrast	Fusion	PET–MRI sensitivity (%)	PET–MRI specificity (%)
Sawicki et al. [29]	2017	Prospective	30	59	70	Pancreas (14), small bowel (12), rectum (1), appendix (1), adrenal glands (1), CUP (1)	NA	DOTATOC	65 ± 11	Dyn	Dyn	3.0	b = 0, 500, 1000	ECA	Simultaneous	NA	NA
Seith et al. [34]	2018	Retrospective	29	57	157	Small bowel (10), pancreas (8), CUP (4), appendix (3), lung (1), stomach (1), ovary (1)	NA	DOTATATE	NA	Dyn	Dyn	3.0	b = 50, 800	No contrast	Simultaneous	NA	NA

Table 1 (continued)

Study	Year of publication	Study design	No. of patients	Patient age mean	Total no. of liver metastases	Primary origin (*n*)	Tumor size (cm)	Type of DOTA-SSA	DOTA-SSA dose, (MBq, range)	CT for fusion	MRI for fusion	MRI magnet field (T)	DWI (*b*, s/mm^2)	MRI contrast	Fusion	PET–MRI sensitivity (%)	PET–MRI specificity (%)
Alshammari et al. [76]	2019	Retrospective	37	56.4	16	Mid gut (14), pancreas (8), lungs (6), CUP (5), paragangliomas (3), mediastinal (1)	≤0.5 cm (*n* = 27) >0.5 cm (*n* = 22)	DOTATOC	150 (138–180)	Dyn	Dyn	3.0	*b* = 0, 400, 800	HBA	Simultaneous	NA	NA
Barachini et al. [36]	2020	Prospective	11	54.6	52	Ileum (7), colon (3), Bauhin valve (1)	≤0.5 cm (*n* = 27) >0.5 cm (*n* = 22)	NA[a]	4	Dyn	Dyn	1.5	*b* = 600	ECA	Simultaneous	96	88
Jawlakh et al. [14]	2021	Prospective	11	59	187	Pancreas (5), small bowel (6)	NA	DOTATOC	2/kg	Dyn	Dyn	3.0	*b* = 0, 50, 800	HBA	Simultaneous	NA	NA

CT computed tomography, *CUP* carcinoma of unknown primary, *Dyn* dynamic contrast-enhanced images, *DWI* diffusion-weighted imaging, *ECA* extracellular contrast agent, *HBA* hepatobiliary contrast agent, *MRI* magnetic resonance imaging, *NA* not applicable, *PV* portal venous phase image

[a]PET/MRI Radiotracer for this original article was ^{18}F-FDOPA

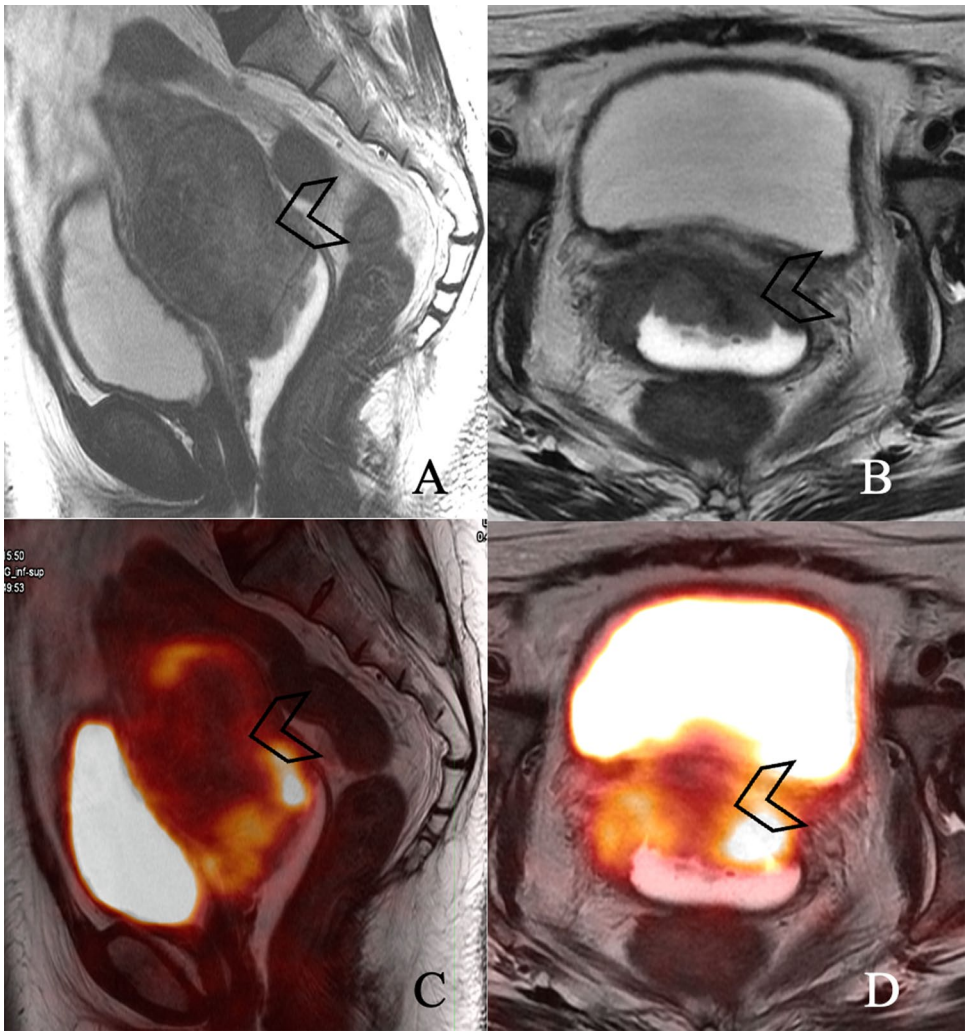

Fig. 2 A 44-year-old woman with poorly differentiated neuroendocrine carcinoma (small cell) of the cervix. **A** Sagittal, **B** axial T2 weighted MRI images, **C** sagittal and **D** axial T2 weighted PETMR images demonstrate a large FDG avid cervical mass (arrowhead) with parametrial extension

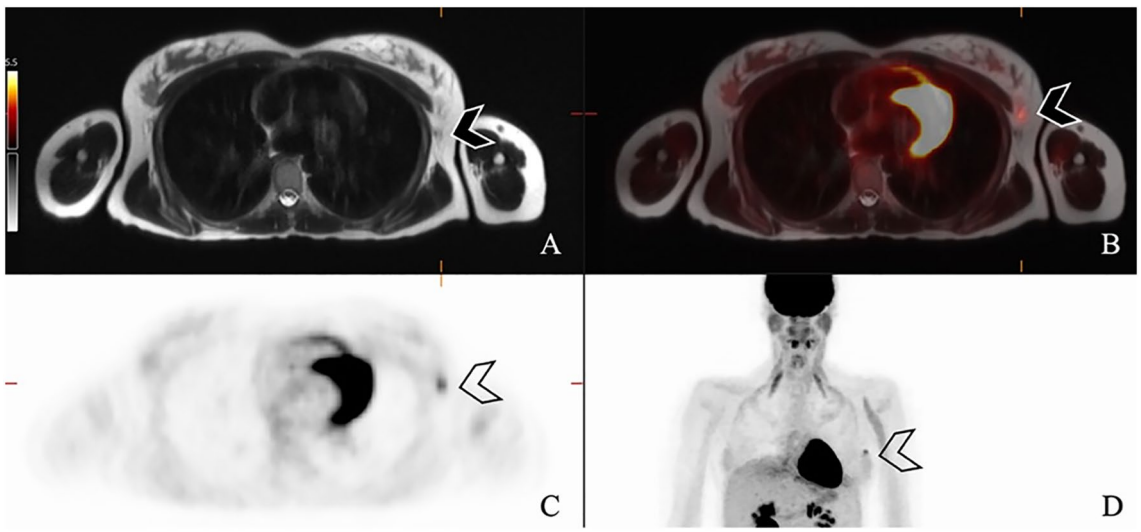

Fig. 3 A 28-year-old pregnant woman was diagnosed with poorly differentiated neuroendocrine carcinoma (small cell) involving the left breast. **A** Axial T2 weighted image shows a small T2 hypointense nodule (arrowhead) in the left breast region. **B** Axial T2 weighted PET/MR image, **C** axial, and **D** attenuation corrected PET images show an FDG avid nodule in the breast region (arrowhead) in keeping with the primary lesion, with no evidence of metastatic disease

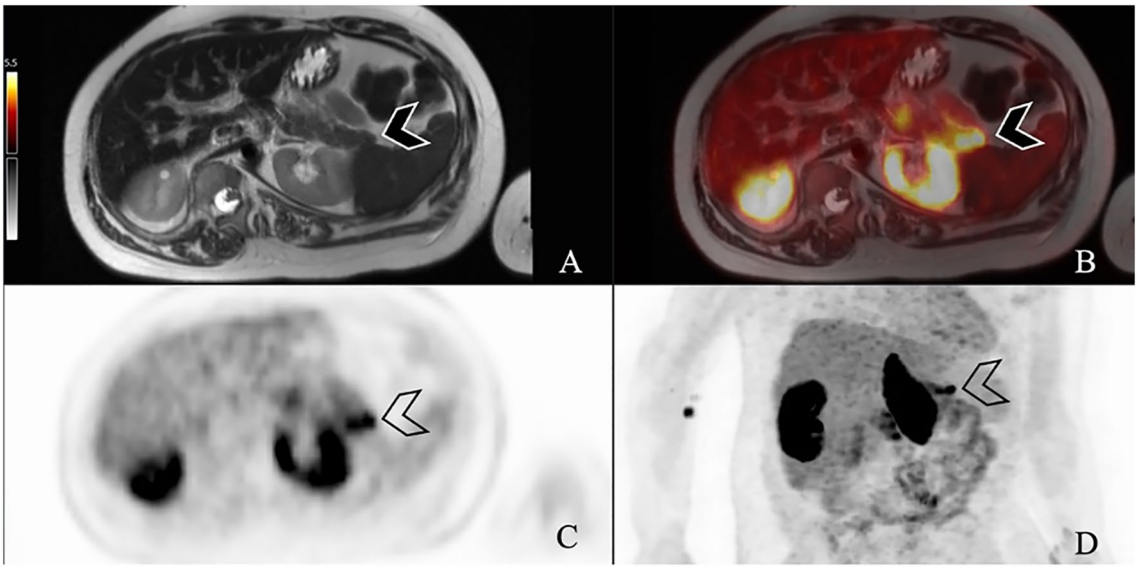

Fig. 4 A 14-year-old boy with hyperinsulinemia is being evaluated for insulinoma. **A** The axial T2 weighted image shows no focal lesion in the pancreatic tail (arrowhead). **B** Axial T2 weighted F-DOPA fused PETMR image, **C** axial, and **D** attenuated corrected PET images demonstrate a small area of intense focal uptake in the pancreatic tail (arrowheads). Findings are consistent with an insulinoma

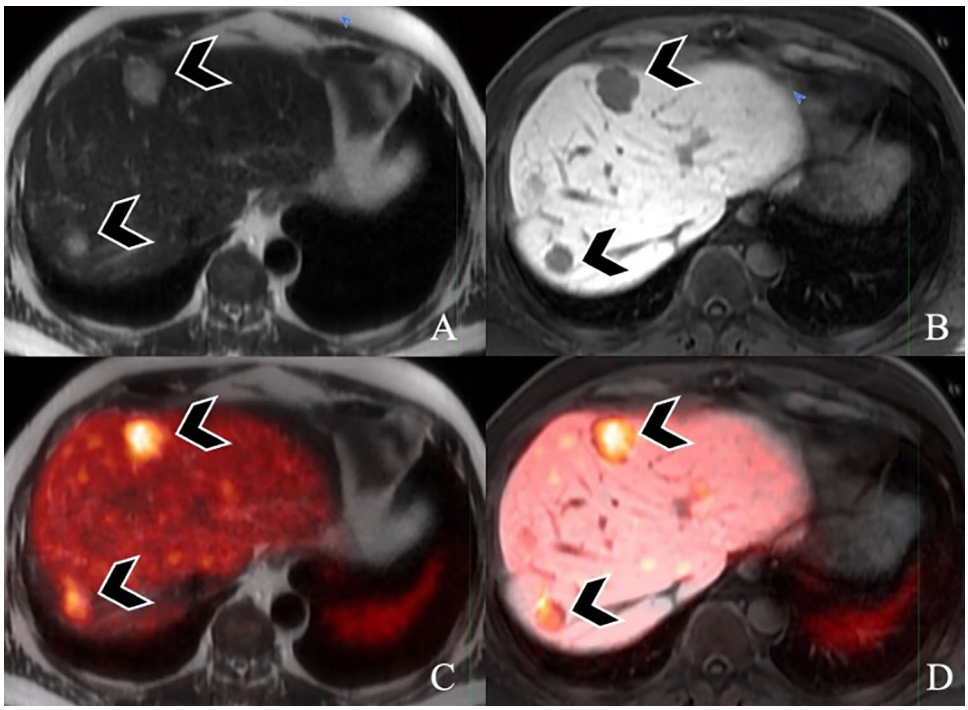

Fig. 5 A 51-year-old male with poorly differentiated neuroendocrine carcinoma (large cell) involving the ileum. **A** Axial T2 weighted, **B** axial T1 weighted MRI images, **C** axial T2 weighted, and **D** axial T1 weighted PETMR images demonstrate avid hepatic metastases (arrowhead)

fast, nonenhanced PET/MRI protocols (T2 haste, T2 TSE, and diffusion-weighted imaging, DWI) with SSTR-PET/CT demonstrated at least comparable effectiveness in overall detection rates in metastatic GEP-NENs and superior detection in metastatic bone and liver lesions [34]. Similar results were found by Alshammari et al., confirming the comparable accuracy in detection and staging as an advantage in characterizing liver lesions [35]. In a study assessing the value of image fusion in PET/MRI compared to standard DWI MRI, fused PET/MRI was superior in detecting liver metastasis [36]. This study also described PET/CT superiority over standard MRI without DWI [36]. Because most patients undergo liver MRI and PET during the routine staging of GEP-NENs and in the assessment of treatment

response, combined PET/MRI, including DWI, has promise as a comprehensive study in managing these tumors. In addition, Beiderwellen et al. conducted a study to evaluate the role of PET–MR enterography in the assessment of intestinal pathologies [37]. They reported high image quality with good co-registration of PET and MRI, enabling high-quality assessment of malignant and inflammatory intestinal lesions.

Radiomics is a rapidly growing field that has shown promise in GEP-NET analysis. A review article by Saleh et al. described radiomics utility in diagnostics, risk stratification, management, and treatment response assessment of pancreatic neuroendocrine tumors [38]. Radiomics, or the extraction of quantitative features from cross-sectional imaging, has been a promising research area for many solid organ malignancies. PET/MRI radiomics has been explored in the literature regarding GEP-NETs, and studies are described in Table 2. In a study utilizing a quantitative 3D assessment of ^{68}Ga-DOTATOC with DWI, a ratio of PET-derived mean SUV and apparent diffusion coefficient (ADC) created a combined variable that could predict grade 2 GEP-NETs with a sensitivity and specificity of 86% and 100%, respectively [39]. PET/MRI textural analysis showed a weak correlation with NENs with low Ki-67 index, but these metrics may be suitable in the high-grade neoplasms [40]. Metrics such as relative T1 weighted hyperintensity (when compared to muscle), arterial phase hyperenhancement, SUV_{max} (when compared to the liver), and diffusion restriction were associated with a more aggressive tumor biology [41]. In a retrospective study by Mapelli et al., second-order radiomic data and SUV parameters demonstrated an ability to predict lymph node involvement in pancreatic NETs with an AUC of 0.992 [42].

A recent meta-analysis was conducted to assess the diagnostic performance of PETMRI for NENs in five studies, with 105 patients reporting equal or superior liver metastases detection by PET/MRI over PET/CT [27]. Another study reported a higher proportion of correct identification of lesions in whole-body staging Ga-DOTATOC PET/MRI of NET patients than ^{68}Ga-DOTATOC PET/CT [29]. Jawlakh et al. reported that the overall tumor detection rate and reader's confidence on PET/MRI with ^{68}Ga-DOTATOC and ^{11}C-5-Hydroxy-tryptophan (^{11}C-5-HTP) were superior to that of ^{68}Ga-DOTATOC-PET/CT for NENs imaging [14]. A study by Berzaczy et al. reported that whole-body ^{68}Ga-DOTANOC PET/MRI appears comparable to ^{68}Ga-DOTANOC PET/CT for detecting distant metastatic disease in patients with well-differentiated NETs [28]. Another study reported that a non-enhanced fast MR protocol comprising T2 HASTE, T2 TSE, and DWI for SSR-PET/MRI had comparable effectiveness in lesion detection as PET/CT [34].

Molecular imaging techniques

There are six different subtypes of SSTRs that are widely expressed in human cells [43]. NENs are a group of tumors with the highest level of SSTR expressions and are present in 80–100% of GEP-NENs [44]. Successful molecular imaging techniques of GEP-NENs utilize this inherent overexpression of somatostatin receptors. GEP-NENs most likely express the 2A subtype SSTR [43]. In the past, the radiopharmaceutical of choice for somatostatin receptor imaging was ^{111}In-pentetreotide (OctreoScan®), used primarily

Table 2 PET/MRI radiomics evaluation of GEP-NETs

Study	Study design	Number of patients	Type of DOTA-SSA	Objective	Result
Bruckmann et al. (2021)	Prospective	26	^{68}Ga-DOTATOC	First order radiomic data: T1w hyperintensity compared to muscle, arterial phase hyperenhancement, diffusion restriction, and SUV_{max} above hepatic level	Odds ratio association with aggressive tumor biology: T1w hyperintensity (12.7), arterial hyper-enhancement (1.4), diffusion restriction (2.8), and SUV_{max} (7.0)
Mapelli et al. (2022)	Retrospective	16	^{68}Ga-DOTATOC	First order radiomic data: SUV_{mean} and SUV_{max} Second order radiomic data: GrayLevelVariance and HighGrayLevelZoneEmphasis	Predicted lymph node involvement: SUV_{mean} (AUC = 0.850) SUV_{max}(AUC 0.783) GrayLevelVariance and HighGrayLevelZoneEmphasis (AUC = 0.992)

PET positron emission tomography, *ADC* apparent diffusion coefficient, *AUC* Area under the ROC curve

[a]DOTATATE gallium (Ga-68) is a somatostatin-2 receptor analog which is radiolabeled with gallium-68 as a positron-emitting radioisotope. Ga-68 DOTATATE has a high affinity for somatostatin-2 receptor and it is rapidly excreted from the nontarget sites which gives it an ideal candidate for imaging neuroendocrine tumors

Table 3 Indications for SSTR-PET

Diagnostics	Treatment planning/surveillance
Baseline staging after histological diagnosis	Selection of patients for PRRT
Localizing lesions in patients with NEN and unknown primary location	Pre-surgical staging
Evaluation of a mass suggestive of NEN but not amenable to tissue sampling	Monitoring of NENs best seen on SSTR-PET
Biochemical evidence of NEN with negative CI	Restaging after completion of PRRT
Restaging for clinical/biochemical progression	
New indeterminate lesion on CI with unclear progression	

SSTR somatostatin receptor, *NEN* neuroendocrine neoplasm, *PRRT* peptide receptor radionucleotide therapy, *CI* conventional imaging

in planar imaging and SPECT [4]. These techniques were replaced for almost all clinical indications (Table 3) following the advent of PET/CT, partially due to the low spatial resolution of images and high false negative rate in organs that exhibit substantial physiologic uptake.

In today's clinical practice, octreoscan has been replaced by ^{64}copper (^{64}Cu) and ^{68}gallium (^{68}Ga) tagged peptides for PET tracers such as -TATE (Tyr3-octreaotate), -TOC (TyI3-octreotide), and -NOC (NaI3-octreotide). Chelation of the molecules with -DOTA (1, 4, 7, 10-tetra-azacyclododecane-1, 4, 7, 10-tetraacetic acid) is conducted in the creation of ^{68}Ga-labeled DOTApeptide octreotide derivatives (DOTATATE, DOTATOC, and DOTANOC) used in imaging [4, 45]. In a study comparing ^{64}Cu-DOTATATE and ^{68}Ga-DOTATOC, ^{64}Cu-DOTATATE had a distinctive advantage in detecting more NET lesions, though both radiotracers had similar patient-based sensitivities [46]. ^{64}Cu-DOTATATE has a longer half-life (12.7 h) and a lower positron range, allowing for increased practicality in a clinical setting and improved image quality, respectively [46]. In a meta-analysis of 416 patients comparing ^{68}Ga-DOTATATE and ^{68}Ga-DOTATOC, their pooled sensitivities for diagnosing NET lesions were 96% and 93%, with specificities at 100% and 85% demonstrating ^{68}Ga-DOTATATE as a more accurate diagnostic radiotracer molecule [47]. Mayerhoefer et al. showed similar performance of gadoxetate-enhanced and diffusion-weighted sequences for ^{68}Ga-DOTATOC PET/MRI in diagnosing intraabdominal neuroendocrine tumors [48]. Newer SSTR agents with a higher affinity for the 2A receptor subset are actively being investigated in the literature. One of these agents, ^{68}Ga-OPS202, has shown promise in terms of safety and sensitivity for detecting neuroendocrine tumors compared with ^{68}Ga-DOTATOC [49].

Tumor scoring systems

Somatostatin receptor analogs used in the imaging of GEP-NETs can be utilized in treating these tumors by linking a therapeutic isotope in place of those used for imaging, a technique termed peptide receptor radionucleotide therapy, PRRT [50]. The Krenning score was initially developed for somatostatin receptor scintigraphy (SRS) to determine whether a patient would be an excellent candidate for this therapy. In the Krenning score, tumors are assigned grades between 1 and 4 based on SSTR tracer uptake relative to background, liver, and spleen activity [51].

A five-point scale titled Somatostatin receptor PET-reporting and data system (SSTR-RADS) was piloted in 2018 by Werner et al. as a standardized objective framework for diagnosing and treatment planning of NENs [52]. Based on tracer uptake patterns, lesions are classified into five groups, 1 (benign) through 5 (almost certainly malignant NET), that ultimately dictate patient management (Table 4). SSTR-RADS guided assessment has demonstrated a high concordance rate amongst readers with varying levels of expertise, indicating the system's versatility and readiness to be implemented/studied on a larger-scale [53]. SSTR-RADS utilizes data on whole tumor burden rather than only comparing the Krenning score's uptake in the lesion of interest to the liver and spleen. SSTR-RADS considers multimodality (conventional cross-sectional and molecular imaging) data when assigning a score to a particular patient.

^{18}F-FDG PET/CT is complementary to SSTR imaging in cases of high-grade and poorly differentiated GEP-NEN. It is typical for low-grade well-differentiated NENs to have little glucose metabolism, though, in 40% of these tumors, FDG uptake can be seen [54]. As dedifferentiation occurs, upregulation of glucose receptors and downregulation of SSTR occurs, termed a "flip-flop phenomenon" [4]. Significant inter and intra-tumoral variation occurs in patients with GEP-NENs. This led to the combined clinical use of both FDG and SSTR-PET to aid in characterizing tumor heterogeneity, risk stratification, and predicting tumor response to PRRT. A NETPET score was developed, combining imaging findings from ^{18}F-FDG and SSTR-PET, which has shown promise as a prognostic biomarker and warrants investigation in future larger studies [55, 56].

Table 4 SSTR-RADS overview

SSTR-RADS category	Findings	Uptake level	Recommendations	Candidate for PRRT?
1 (Benign)	Known benign lesions (biopsy proven or pathognomonic on CI)			No
1A	Benign lesion, characterized by biopsy or in accordance with imaging and no abnormal uptake	1		No
1B	Benign lesion characterized by biopsy or in accordance with imaging but exhibits focal increased uptake	2–3		No
2 (Likely benign)	Low level or nonspecific SSTR uptake at site atypical for NET metastasis	1		No
3 (Indeterminate)	Findings that are suggestive of but not definitive for NEN		Further workup indicated	
3A	Equivocal uptake in soft tissue sites typical for NET metastasis	1–2	Biopsy or 3 month follow-up imaging	No
3B	Bone uptake that is not atypical for NET	1–2	3 month follow-up imaging	Yes (if multiple)
3C	Suggestive of an SSTR expressing, non-NET benign tumor or malignant process	3	Biopsy	No
3D	Highly suspicious of malignant NEN, but no SSTR uptake		^{18}F-FDG PET may be of further value	No
4 (NET highly likely)	Intense tracer uptake in a typical location without common features on CI	3	No biopsy needed	Yes
5 (NET almost certain)	Intense tracer uptake in a typical location with corresponding CI features	3	Negative biopsy likely false negative	Yes

Levels of uptake: 1: less than or equal to blood pool, 2: greater than blood pool but less than or equal to the liver, and 3: greater than the liver

SSTR-RADS somatostatin receptor PET-reporting and data system, *PRRT* peptide receptor radionucleotide therapy, *CI* conventional imaging, *NET* neuroendocrine tumor

PRRT and monitoring treatment response

PRRT is a tailored therapeutic technique that utilizes the specific biological activity of the targeted lesion. The National Comprehensive Cancer Network (NCCN) endorsed the use of SSTR imaging in determining patients' eligibility to receive PRRT [57]. Only patients with tumors showing adequate expression of SSTR, typically a Krenning score of greater than 2, are eligible to receive this therapy [58].

The development of criteria for determining response to therapy is challenging due to the heterogeneity of NENs and slow growth rate [59]. The WHO and ENETS classification systems, which were widely popularized, lacked large data registries for analysis and did not account for tumor heterogeneity [60]. Additional criteria, such as the Response Evaluation Criteria in Solid Tumors (RECIST) and the modified RECIST, have limitations when describing slow-growing tumors, particularly those with small volume, inflammatory characteristics, fibrosis, or hemorrhage [60, 61]. Multigene liquid biopsy (NETest) is a blood-based biomarker detection system that analyzes 51 circulating mRNA sequences that are common in GEP-NENs [4]. The test involves a dual-step protocol (mRNA isolation, cDNA production, and polymerase chain reaction) from EDTA-collected whole blood. In addition, it utilizes mathematical tools such as a support vector machine, linear discriminant analysis, *k*-nearest neighbors, and the naïve Bayes algorithm. The test successfully identifies eight biologically relevant genes "omic" clusters (SSTRome, proliferome, signalome, metabolome, secretome, epigenome, plurome, and apoptome), which define the tumor fingerprint and constitute the oncobiome of the cell [62]. The clinical interpretation of this information is presented as a diagnostic score ranging from 0% (low activity) to 100% (high activity). The utilization of NETest has been demonstrated in the literature to have a high accuracy in determining treatment response in GEP-NETs, predicting recurrence following surgical resection [59, 60, 63–66]. Few studies have evaluated the role of the standardized uptake value (SUV) parameter of ^{68}Ga-DOTATATE PET/CT in predicting PFS and response to the treatment [67, 68]. The mean SUV_{max} was significantly higher in responders than non-responders [67, 68] and was higher in patients with PFS > 18 months [68]. A study involving 128 patients with NENs of all WHO grades reported that ^{64}Cu-DOTATATE SUV_{max} in tumor lesions was significantly associated with the PFS [69].

Table 5 Advantages and weaknesses of PET/MRI

Advantages	Weakness
Improved lesion detection in the brain, breast, liver, kidneys, and bone	Increase acquisition time
Better alignment of simultaneously acquired PET–MRI data compared to PET–CT	Limited availability
Improved quantifications by MRI-based motion correction without additional radiation	High capital cost
No ionizing radiation	Lack of standardized protocol
Single appointment for patient who requires both PET and MRI	Limited evaluation of smaller pulmonary nodules and osseous lesions
Expanded capabilities with multiparametric sequences such as DWI, perfusion MRI and spectroscopy	Special training to technologists
	Lack of reimbursement

PET/MRI challenges

Understanding the pitfalls of SSTR imaging is essential because of its effect on imaging interpretation and, ultimately, patient care Table 5. The spleen exhibits the highest amount of physiologic uptake of ^{68}Ga-DOTATATE and, to a lesser degree, the liver, kidneys, adrenals, stomach, prostate, and small intestine [39]. Of note, it is common to encounter patients with physiologic tracer uptake in the uncinate process and tail of the pancreas [70]. Physiological uptake in this area can usually be differentiated from tumor due to its more diffuse and elongated appearance rather than a focal area of tracer activity. Though, in some cases, this may be a difficult distinction to make. A study utilizing dynamic PET/CT acquisition in calculating the net influx (Ki) successfully differentiated physiological uptake in the uncinate process from pancreatic neuroendocrine tumors [70]. The liver is a common primary location for NEN metastasis. Physiologic uptake of SSTR compounds may hide underlying metastatic liver lesions. Using hepatobiliary-specific contrast agents such as gadoxetate disodium can aid in identifying GEP-NET hepatic metastasis with high sensitivity [20, 48, 71, 72]. PET/MRI has a low sensitivity for detecting bone lesions largely because MRI attenuation techniques may underestimate tracer uptake values in densely sclerotic lesions [73]. In addition, MRI is less sensitive in detecting pulmonary lesions due to the low resolution of the lung parenchyma [16, 74].

Several issues have arisen which have limited the use of PET/MRI. Acquiring PET/MRI requires technologists to have dual training in PET and MRI. Having two technologists present, each with one of these two proficiencies may solve this problem but will be more costly. Another issue relates to the lack of reimbursement for PET/MRI services. There is also no specific Current Procedural Terminology (CPT®) codes for PET/MRI. As such, this requires submitting individual codes for whole-body PET and MRI. In a European study of the management and cost considerations between PET/CT and PET/MRI, PET/MRI costs 50% more per examination [75]. This study demonstrated that PET/MRI provides additional clinical value in changes to more appropriate management in 8% of cancer patients who undergo PET/CT in routine clinical practice [75]. Patient comfort is another consideration in PET/MRI, with the modality having longer image acquisition times. Optimization of PET/MRI protocols can aid in overcoming this time constraint.

Future perspectives and trials

A list of the currently ongoing clinical trials regarding the diagnostic utility of PET/MRI in neuroendocrine tumors can be found in Table 6. These trials are recruiting participants as of the time of writing this manuscript and hopefully will provide better larger-scale data regarding the use of PET/MRI in patients with NETs.

Conclusion

The advent of advanced molecular imaging techniques has led to improvement in diagnostic abilities and patient prognosis in those affected with solid organ malignancies. SSTR-PET/MRI has shown promise in the diagnosis, staging, and treatment assessment of GEP-NETs, especially those with hepatic involvement. The utilization of hepatobiliary-specific contrast agents is key to accurate diagnostic abilities for these tumors. There is a shortcoming of PET/MRI regarding detecting sclerotic bony and lung lesions; for those cases, PET/CT is superior. Advances in MRI radiomics have shown promise in the preoperative staging of GEP-NETs. PET/MRI does not come without challenges. Technical requirements for imaging acquisition, reimbursement coding, and scan time must be considered when utilizing PET/MRI services.

Table 6 PET/MRI clinical trials for Neuroendocrine tumors

ClinicalTrials.gov Identifier	Recruitment status	Location (sponsor/collaborator/country)	Study design (study type/actual enrollment)	Official title	Outcome measure (primary outcome)	Outcome measure (secondary outcome)
NCT03145857	Recruiting	AHS Cancer Control Alberta/not provided/Canada	Interventional/500 participants	A phase I/II study of gallium-68 HA-DOTATATE [68]Ga-HA-DOTATATE)[a] in patients with known or suspected somatostatin receptor positive tumours	Change in vital signs following injection of [68]Ga-HA-DOTATATE[a], where vital signs are measured before and after injection of [68]Ga-HA-DOTATATE[a], and changes are summarized. Changes in hematology and SMA-12 serum biochemistry following administration of [68] Ga-HA-DOTATATE. Once [68] Ga-HA-DOTATATE[a] has been administered, all participants will be examined for the occurrence of adverse events (AEs) within 24 h, as well as the correlation of [68] Ga-HA-DOTATATE[a] scan with standard of care cross-sectional imaging and published data	Evaluation of [68] Ga-HA-DOTATATE[a] scan changes compared to baseline scan. Applicable, follow-up [68] Ga-HA-DOTATATE[a] scans will be evaluated for abnormal accumulation of [68] Ga-HA-DOTATATE. The maximum standardized uptake value (SUV_{max}) will be determined for the target lesions identified at baseline and compared to the results of the baseline [68]Ga-HA-DOTATATE[a]. An overall assessment of the correlation between the follow-up and baseline scan will be made
NCT03918759	Recruiting	Massimo Falconi, IRCCS San Raffaele/IRCCS San Raffaele/Italy	Observational/150 participants	Diagnostic accuracy of 68gallium positron emission tomography/magnetic resonance imaging (68Ga PET/MRI), endoscopic ultrasound (EUS) and computed tomography in the assessment of lymph node metastases by nonfunctioning pancreatic neuroendocrine neoplasms	Accuracy of preoperative staging in detecting nodal metastases by evaluating and comparing sensitivity and specificity of the diagnostic techniques	The secondary outcomes include the assessment of the prognostic role of nodal involvement on disease/progression free survival in patients who undergo a pancreatic resection for a non-functioning pancreatic neoplasms. This secondary outcome include the evaluation of other possible variables that can be associated with the risk of nodal metastases such as preoperative dimension in mm of the PanNEN, location, features at the imaging, standard uptake value (SUV)

Table 6 (continued)

ClinicalTrials.gov Identifier	Recruitment status	Location (sponsor/collaborator/country)	Study design (study type/actual enrollment)	Official title	Outcome measure (primary outcome)	Outcome measure (secondary outcome)
NCT04045834	Recruiting	Xiaoli Lan, Wuhan Union Hospital, China/not provided/China	Observational/ 60 participants	Study of the diagnostic value of hybrid PET/MR and PET/CT in neuroendocrine diseases and tumor-induced osteomalacia	Sensitivity and specificity of diagnosis and staging. The presence of non-physiological uptake or uptake in a tissue structure can be considered pathological. The signal intensity of PET indicates the presence and density of SSTR in the tissue. The lesion intake is higher than the liver and is classified as clearly positive. The lesion and the surrounding normal tissue ROI, measure the SUV, and calculate the T/B ratio. Special attention should be paid to the analysis of the causes of false positives and false negative results	Not provided
NCT04081701	Recruiting	Weill Medical College of Cornell University/ Novartis Pharmaceuticals/ United States	Observational/90 participants	68Ga (gallium)-DOTATATE[a] positron emission tomography (PET)/MRI in the diagnosis and management of somatostatin receptor positive central nervous system CNS tumors	Evaluate whether Ga-68-DOTATATE[a] PET/MRI provides additional clinical benefit. Diagnostic accuracy of Ga-68-DOTATATE PET/MRI will be compared to MRI alone. Correlative analyses will be performed including logistic regression/ Spearman correlation for continuous variables, and Mann–Whitney *U* tests for not normally distributed subgroups for variables allowing for dichotomization	Correlate Ga-68-DOTATATE[a] PET/MR findings with histopathologic biomarkers, SSTR2, Ki67, progesterone receptor, epidermal growth factor (EGFR) expression

PET positron emission tomography, *MR* magnetic resonance, *PanNEM* pancreatic neuroendocrine neoplasm, *ROI* region of interest, *SSTR2* somatostatin receptor 2, *Ki67* antigen Ki67, *EGFR* epidermal growth factor

[a]DOTATATE gallium (Ga-68) is a somatostatin-2 receptor analog radiolabeled with gallium-68 as a positron-emitting radioisotope. Ga-68 DOTATATE has a high affinity for the somatostatin-2 receptor, rapidly excreted from the nontarget sites, making it an ideal candidate for imaging neuroendocrine tumors

PET/MRI offers the potential to become a comprehensive modality for GEP-NET imaging. However, future studies using novel radiotracers, radiomic trending, and a more considerable population prospective analysis demonstrating efficacy are warranted to solidify the modalities used on a widespread scale.

Author contributions All authors contributed to this paper with the conception and design of the study, literature review and analysis, drafting and critical revision and editing, and final approval of the final version.

Funding No financial support/funding.

References

1. Ambrosini, V., et al., *Consensus on molecular imaging and theranostics in neuroendocrine neoplasms.* Eur J Cancer, 2021. **146**: p. 56–73.
2. Taal, B.G. and O. Visser, *Epidemiology of neuroendocrine tumours.* Neuroendocrinology, 2004. **80 Suppl 1**: p. 3–7.
3. Oronsky, B., et al., *Nothing But NET: A Review of Neuroendocrine Tumors and Carcinomas.* Neoplasia, 2017. **19**(12): p. 991–1002.
4. Rajamohan, N., et al., *PET/CT and PET/MRI in neuroendocrine neoplasms.* Abdom Radiol (NY), 2022.
5. Crona, J. and B. Skogseid, *GEP- NETS UPDATE: Genetics of neuroendocrine tumors.* Eur J Endocrinol, 2016. **174**(6): p. R275–90.
6. Xu, Z., et al., *Epidemiologic Trends of and Factors Associated With Overall Survival for Patients With Gastroenteropancreatic Neuroendocrine Tumors in the United States.* JAMA Network Open, 2021. **4**(9): p. e2124750.
7. Kawasaki, K., M. Fujii, and T. Sato, *Gastroenteropancreatic neuroendocrine neoplasms: genes, therapies and models.* Dis Model Mech, 2018. **11**(2).
8. Rindi, G., G. Petrone, and F. Inzani, *The 2010 WHO classification of digestive neuroendocrine neoplasms: a critical appraisal four years after its introduction.* Endocr Pathol, 2014. **25**(2): p. 186–92.
9. Yang, M., et al., *Evaluation of the World Health Organization 2010 grading system in surgical outcome and prognosis of pancreatic neuroendocrine tumors.* Pancreas, 2014. **43**(7): p. 1003–8.
10. Morin, E., et al., *Hormone profiling, WHO 2010 grading, and AJCC/UICC staging in pancreatic neuroendocrine tumor behavior.* Cancer Med, 2013. **2**(5): p. 701–11.
11. Liu, T.C., et al., *Comparison of WHO Classifications (2004, 2010), the Hochwald grading system, and AJCC and ENETS staging systems in predicting prognosis in locoregional well-differentiated pancreatic neuroendocrine tumors.* Am J Surg Pathol, 2013. **37**(6): p. 853–9.
12. Zamora, V., et al., *Immunohistochemical expression of somatostatin receptors in digestive endocrine tumours.* Dig Liver Dis, 2010. **42**(3): p. 220–5.
13. Pirasteh, A., et al., *PET/MRI for neuroendocrine tumors: a match made in heaven or just another hype?* Clin Transl Imaging, 2019. **7**(6): p. 405–413.
14. Jawlakh, H., et al., *^{68}Ga-DOTATOC-PET/MRI and 11C-5-HTP-PET/MRI are superior to ^{68}Ga-DOTATOC-PET/CT for neuroendocrine tumour imaging.* Journal of Neuroendocrinology, 2021. **33**(6): p. e12981.
15. Ehman, E.C., et al., *PET/MRI: Where might it replace PET/CT?* J Magn Reson Imaging, 2017. **46**(5): p. 1247–1262.
16. Galgano, S.J., et al., *Applications of PET/MRI in Abdominopelvic Oncology.* Radiographics, 2021. **41**(6): p. 1750–1765.
17. Miles, K.A., S.A. Voo, and A.M. Groves, *Additional clinical value for PET/MRI in oncology: moving beyond simple diagnosis.* Journal of Nuclear Medicine, 2018. **59**(7): p. 1028–1032.
18. Cabello, J. and S.I. Ziegler, *Advances in PET/MR instrumentation and image reconstruction.* Br J Radiol, 2018. **91**(1081): p. 20160363.
19. Hope, T.A., et al., *Simultaneous $^{(68)}$Ga-DOTA-TOC PET/MRI with gadoxetate disodium in patients with neuroendocrine tumor.* Abdom Imaging, 2015. **40**(6): p. 1432–40.
20. Panda, A., et al., *PET/Magnetic Resonance Imaging Applications in Abdomen and Pelvis.* Magn Reson Imaging Clin N Am, 2020. **28**(3): p. 369–380.
21. Catana, C., *Motion correction options in PET/MRI.* Semin Nucl Med, 2015. **45**(3): p. 212–23.
22. Lalush, D.S., *Magnetic Resonance-Derived Improvements in PET Imaging.* Magn Reson Imaging Clin N Am, 2017. **25**(2): p. 257–272.
23. Fuin, N., et al., *Concurrent Respiratory Motion Correction of Abdominal PET and Dynamic Contrast-Enhanced-MRI Using a Compressed Sensing Approach.* J Nucl Med, 2018. **59**(9): p. 1474–1479.
24. Izquierdo-Garcia, D., et al., *Comparison of MR-based attenuation correction and CT-based attenuation correction of whole-body PET/MR imaging.* Eur J Nucl Med Mol Imaging, 2014. **41**(8): p. 1574–84.
25. Martinez-Möller, A., et al., *Workflow and scan protocol considerations for integrated whole-body PET/MRI in oncology.* Journal of Nuclear Medicine, 2012. **53**(9): p. 1415–1426.
26. Martin, S., et al., *Neuroendocrine neoplasm imaging: protocols by site of origin.* Abdominal Radiology, 2022: p. 1–15.
27. Choi, S.J., et al., *Diagnostic value of [$^{(68)}$Ga]Ga-DOTA-labeled-somatostatin analogue PET/MRI for detecting liver metastasis in patients with neuroendocrine tumors: a systematic review and meta-analysis.* Eur Radiol, 2022. **32**(7): p. 4628–4637.
28. Berzaczy, D., et al., *Whole-Body ^{68}Ga-DOTANOC PET/MRI Versus ^{68}Ga-DOTANOC PET/CT in Patients With Neuroendocrine Tumors: A Prospective Study in 28 Patients.* Clin Nucl Med, 2017. **42**(9): p. 669–674.
29. Sawicki, L.M., et al., *Evaluation of ^{68}Ga-DOTATOC PET/MRI for whole-body staging of neuroendocrine tumours in comparison with ^{68}Ga-DOTATOC PET/CT.* European Radiology, 2017. **27**(10): p. 4091–4099.
30. Schreiter, N.F., et al., *Evaluation of the potential of PET–MRI fusion for detection of liver metastases in patients with neuroendocrine tumours.* Eur Radiol, 2012. **22**(2): p. 458–67.
31. Hayoz, R., et al., *The combination of hepatobiliary phase with Gd-EOB-DTPA and DWI is highly accurate for the detection and characterization of liver metastases from neuroendocrine tumor.* Eur Radiol, 2020. **30**(12): p. 6593–6602.
32. Tirumani, S.H., et al., *Value of hepatocellular phase imaging after intravenous gadoxetate disodium for assessing hepatic metastases from gastroenteropancreatic neuroendocrine tumors: comparison with other MRI pulse sequences and with extracellular agent.* Abdominal Radiology, 2018. **43**(9): p. 2329–2339.
33. Morse, B., et al., *Magnetic Resonance Imaging of Neuroendocrine Tumor Hepatic Metastases: Does Hepatobiliary Phase Imaging Improve Lesion Conspicuity and Interobserver Agreement of Lesion Measurements?* Pancreas, 2017. **46**(9).
34. Seith, F., et al., *Fast non-enhanced abdominal examination protocols in PET/MRI for patients with neuroendocrine tumors (NET): comparison to multiphase contrast-enhanced PET/CT.* La radiologia medica, 2018. **123**(11): p. 860–870.

35. Alshaima Alshammari, M.M., Rizwan Syed, Evangelia Skoura, Sofia Michopoulou, Fulvio Zaccagna, Jamshed Bomanji, Francesco Fraioli, *Impact of Integrated Whole Body ^{68}Ga PET/MR Imaging in Comparison with ^{68}Ga PET/CT in Lesions Detection and Diagnosis of Suspected Neuroendocrine Tumours.* American Journal of Internal Medicine, 2019. **7**(4).
36. Barachini, O., et al., *The impact of ^{18}F-FDOPA-PET/MRI image fusion in detecting liver metastasis in patients with neuroendocrine tumors of the gastrointestinal tract.* BMC Med Imaging, 2020. **20**(1): p. 22.
37. Beiderwellen, K., et al., *Hybrid imaging of the bowel using PET/MR enterography: Feasibility and first results.* European Journal of Radiology, 2016. **85**(2): p. 414–421.
38. Saleh, M., et al., *New frontiers in imaging including radiomics updates for pancreatic neuroendocrine neoplasms.* Abdom Radiol (NY), 2022. **47**(9): p. 3078–3100.
39. Adams, L.C., et al., *Quantitative 3D Assessment of $^{(68)}$Ga-DOTATOC PET/MRI with Diffusion-Weighted Imaging to Assess Imaging Markers for Gastroenteropancreatic Neuroendocrine Tumors: Preliminary Results.* J Nucl Med, 2020. **61**(7): p. 1021–1027.
40. Weber, M., et al., *Textural analysis of hybrid DOTATOC-PET/MRI and its association with histological grading in patients with liver metastases from neuroendocrine tumors.* Nucl Med Commun, 2020. **41**(4): p. 363–369.
41. Bruckmann, N.M., et al., *Correlation between contrast enhancement, standardized uptake value (SUV), and diffusion restriction (ADC) with tumor grading in patients with therapy-naive neuroendocrine neoplasms using hybrid $^{(68)}$Ga-DOTATOC PET/MRI.* Eur J Radiol, 2021. **137**: p. 109588.
42. Mapelli, P., et al., *$^{(68)}$Ga-DOTATOC PET/MR imaging and radiomic parameters in predicting histopathological prognostic factors in patients with pancreatic neuroendocrine well-differentiated tumours.* Eur J Nucl Med Mol Imaging, 2022. **49**(7): p. 2352–2363.
43. Remes, S.M., et al., *Immunohistochemical Expression of Somatostatin Receptor Subtypes in a Panel of Neuroendocrine Neoplasias.* J Histochem Cytochem, 2019. **67**(10): p. 735–743.
44. Reubi, J.C., *Somatostatin and other Peptide receptors as tools for tumor diagnosis and treatment.* Neuroendocrinology, 2004. **80 Suppl 1**: p. 51–6.
45. Pauwels, E., et al., *Somatostatin receptor PET ligands - the next generation for clinical practice.* Am J Nucl Med Mol Imaging, 2018. **8**(5): p. 311–331.
46. Johnbeck, C.B., et al., *Head-to-Head Comparison of $^{(64)}$Cu-DOTATATE and $^{(68)}$Ga-DOTATOC PET/CT: A Prospective Study of 59 Patients with Neuroendocrine Tumors.* J Nucl Med, 2017. **58**(3): p. 451–457.
47. Yang, J., et al., *Diagnostic role of Gallium-68 DOTATOC and Gallium-68 DOTATATE PET in patients with neuroendocrine tumors: a meta-analysis.* Acta Radiol, 2014. **55**(4): p. 389–98.
48. Mayerhoefer, M.E., et al., *Gadoxetate-enhanced versus diffusion-weighted MRI for fused Ga-68-DOTANOC PET/MRI in patients with neuroendocrine tumours of the upper abdomen.* Eur Radiol, 2013. **23**(7): p. 1978–85.
49. Nicolas, G.P., et al., *Sensitivity Comparison of $^{(68)}$Ga-OPS202 and $^{(68)}$Ga-DOTATOC PET/CT in Patients with Gastroenteropancreatic Neuroendocrine Tumors: A Prospective Phase II Imaging Study.* J Nucl Med, 2018. **59**(6): p. 915–921.
50. Mittra, E.S., *Neuroendocrine Tumor Therapy: $^{(177)}$Lu-DOTATATE.* AJR Am J Roentgenol, 2018. **211**(2): p. 278–285.
51. Park, S., et al., *Somatostatin Receptor Imaging and Theranostics: Current Practice and Future Prospects.* J Nucl Med, 2021. **62**(10): p. 1323–1329.
52. Werner, R.A., et al., *SSTR-RADS Version 1.0 as a Reporting System for SSTR PET Imaging and Selection of Potential PRRT Candidates: A Proposed Standardization Framework.* J Nucl Med, 2018. **59**(7): p. 1085–1091.
53. Werner, R.A., et al., *High Interobserver Agreement for the Standardized Reporting System SSTR-RADS 1.0 on Somatostatin Receptor PET/CT.* J Nucl Med, 2021. **62**(4): p. 514–520.
54. Garin, E., et al., *Predictive value of ^{18}F-FDG PET and somatostatin receptor scintigraphy in patients with metastatic endocrine tumors.* J Nucl Med, 2009. **50**(6): p. 858–64.
55. Hindie, E., *The NETPET Score: Combining FDG and Somatostatin Receptor Imaging for Optimal Management of Patients with Metastatic Well-Differentiated Neuroendocrine Tumors.* Theranostics, 2017. **7**(5): p. 1159–1163.
56. Chan, D.L., et al., *Dual Somatostatin Receptor/FDG PET/CT Imaging in Metastatic Neuroendocrine Tumours: Proposal for a Novel Grading Scheme with Prognostic Significance.* Theranostics, 2017. **7**(5): p. 1149–1158.
57. Shah, M.H., et al., *Neuroendocrine and Adrenal Tumors, Version 2.2021, NCCN Clinical Practice Guidelines in Oncology.* J Natl Compr Canc Netw, 2021. **19**(7): p. 839–868.
58. Hope, T.A., et al., *NANETS/SNMMI Consensus Statement on Patient Selection and Appropriate Use of $^{(177)}$Lu-DOTATATE Peptide Receptor Radionuclide Therapy.* J Nucl Med, 2020. **61**(2): p. 222–227.
59. Roll, W., et al., *Imaging and liquid biopsy in the prediction and evaluation of response to PRRT in neuroendocrine tumors: implications for patient management.* Eur J Nucl Med Mol Imaging, 2021. **48**(12): p. 4016–4027.
60. Malczewska, A., et al., *The clinical applications of a multigene liquid biopsy (NETest) in neuroendocrine tumors.* Adv Med Sci, 2020. **65**(1): p. 18–29.
61. Galgano, S.J., et al., *Imaging of Neuroendocrine Neoplasms: Monitoring Treatment Response-AJR Expert Panel Narrative Review.* AJR Am J Roentgenol, 2022. **218**(5): p. 767–780.
62. Modlin, I.M., et al., *The NETest: The Clinical Utility of Multigene Blood Analysis in the Diagnosis and Management of Neuroendocrine Tumors.* Endocrinol Metab Clin North Am, 2018. **47**(3): p. 485–504.
63. Modlin, I.M., et al., *The clinical utility of a novel blood-based multi-transcriptome assay for the diagnosis of neuroendocrine tumors of the gastrointestinal tract.* Am J Gastroenterol, 2015. **110**(8): p. 1223–32.
64. Oberg, K., et al., *A meta-analysis of the accuracy of a neuroendocrine tumor mRNA genomic biomarker (NETest) in blood.* Ann Oncol, 2020. **31**(2): p. 202–212.
65. Modlin, I.M., et al., *Molecular Genomic Assessment Using a Blood-based mRNA Signature (NETest) is Cost-effective and Predicts Neuroendocrine Tumor Recurrence With 94% Accuracy.* Ann Surg, 2021. **274**(3): p. 481–490.
66. Modlin, I.M., et al., *Early Identification of Residual Disease After Neuroendocrine Tumor Resection Using a Liquid Biopsy Multigenomic mRNA Signature (NETest).* Ann Surg Oncol, 2021. **28**(12): p. 7506–7517.
67. Kaewput, C., S. Suppiah, and S. Vinjamuri, *Correlation between Standardized Uptake Value of $^{(68)}$Ga-DOTA-NOC Positron Emission Tomography/Computed Tomography and Pathological Classification of Neuroendocrine Tumors.* World J Nucl Med, 2018. **17**(1): p. 34–40.
68. Teker, F. and U. Elboga, *Is SUV_{max} a useful marker for progression-free survival in patients with metastatic GEP-NET receiving $^{(177)}$Lu-DOTATATE therapy?* Hell J Nucl Med, 2021. **24**(2): p. 122–131.
69. Carlsen, E.A., et al., *$^{(64)}$Cu-DOTATATE PET/CT and Prediction of Overall and Progression-Free Survival in Patients with Neuroendocrine Neoplasms.* J Nucl Med, 2020. **61**(10): p. 1491–1497.

70. Thuillier, P., et al., *Diagnostic performance of a whole-body dynamic ^{68}GA-DOTATOC PET/CT acquisition to differentiate physiological uptake of pancreatic uncinate process from pancreatic neuroendocrine tumor.* Medicine (Baltimore), 2020. **99**(33): p. e20021.
71. Broski, S.M., et al., *Clinical PET/MRI: 2018 Update.* AJR Am J Roentgenol, 2018. **211**(2): p. 295–313.
72. Giesel, F.L., et al., *Comparison of neuroendocrine tumor detection and characterization using DOTATOC-PET in correlation with contrast enhanced CT and delayed contrast enhanced MRI.* Eur J Radiol, 2012. **81**(10): p. 2820–5.
73. Samarin, A., et al., *PET/MR imaging of bone lesions--implications for PET quantification from imperfect attenuation correction.* Eur J Nucl Med Mol Imaging, 2012. **39**(7): p. 1154–60.
74. Antoch, G., et al., *Whole-body dual-modality PET/CT and whole-body MRI for tumor staging in oncology.* JAMA, 2003. **290**(24): p. 3199–206.
75. Mayerhoefer, M.E., et al., *PET/MRI versus PET/CT in oncology: a prospective single-center study of 330 examinations focusing on implications for patient management and cost considerations.* Eur J Nucl Med Mol Imaging, 2020. **47**(1): p. 51–60.
76. Alshammari, A. and M. Masoomi, *Impact of Integrated Whole Body ^{68}Ga PET/MR Imaging in Comparison with ^{68}Ga PET/CT in Lesions Detection and Diagnosis of Suspected Neuroendocrine Tumours.* 2019.